Phase-matching analysis of four-wave mixing induced by modulation instability in a single-mode fiber*

Chen Wei(陈 伟), Meng Zhou(孟 洲)†, and Zhou Hui-Juan(周会娟)

Department of Optic Information Science and Technology, College of Optoelectronic Science and Engineering, National University of Defense Technology, Changsha 410073, *China*

(Received 8 March 2012; revised manuscript received 1 April 2012)

Four-wave mixing induced by modulation instability in a single-mode fiber is analyzed from the phase-matching point of view. For the two-channel transmission, a method is proposed to select the four-wave-mixing-induced sidebands, which is based on the proper use of a continuous-wave and a pulse as light sources. We find that a mass of sidebands are generated in the modulation instability resonance region, and the power of the sideband increases with not only the peak power of the pump pulse but also the continuous-wave power which acts as a seed. The research will be guidable for the fiber communication and sensing systems using the wavelength division multiplexing technology.

Keywords: four-wave mixing, modulation instability, phase matching

PACS: 42.65.–k, 42.65.Sf, 42.81.–i **DOI:** 10.1088/1674-1056/21/9/094215

1. Introduction

Modulation instability (MI) is a significant nonlinear effect in the fiber, which manifests itself in the generation of two symmetric sidebands in the spectrum. It can be treated as a four-wave mixing (FWM) process with the phase matched through self-phase modulation (SPM).[1] The occurrence of this kind of MI needs anomalous dispersion, i.e., the operation wavelength lies in the anomalous dispersion region, which is available for the 1.55-μm transmission in the usual single-mode fiber (SMF). With the development of the wavelength division multiplexing (WDM), FWM among signal channels has attracted more attention as it introduces considerable crosstalk to the system.[2−9] It has been indicated that the FWM efficiency decreases with the fiber dispersion.[10,11] Both FWM and MI cause severe power penalty because of the energy transfer from the pump to the newly generated sidebands, which limits the transmission distance of the system.[12,13] Moreover, a mass of phase noise will also be introduced due to the spectral broadening caused by MI. This is crucial for an interferometric fiber sensing system, because the phase noise decides the detecting resolution. For a special case, in the so-called modulation instability resonance (MIR) region, the channel spacing is close to the MI frequency f_{MI} (corresponding to the maximum gain of MI). As a result of MIR, the FWM interactions between the two signal channels are advanced. It was found that signal depletion is resonantly enhanced in the MIR region, becoming the main source of system performance degradation.[14−17] Therefore, it is significant to have a thorough understanding of MIR, especially in the practical WDM system using SMF generally.

In the past research work, Grosz *et al.* investigated the system impairments induced by MIR in the dispersion shifted fiber (DSF).[15] Here, we will focus on the usual SMF with higher fiber dispersion. As it will be shown in the present paper, the MIR is also notable in the usual SMF in despite of a lower FWM efficiency caused by a higher dispersion. We change the channel spacing as well as the laser power to study the spectral variations in the presence of MIR. We also explain the experimental results from the phase-matching point of view. In order to verify this view more clearly, we utilize a continuous-wave (CW) and a pulse as the laser sources of the two channels. Our research will provide a good guidance for the practical applications of the WDM systems.

*Project supported by the National Natural Science Foundation of China (Grant No. 61177073), the Specialized Research Fund for the Doctoral Program of Higher Education of China (Grant No. 20104307110020), the Fund of Innovation of Graduate School of National University of Defense Technology, China (Grant No. B110703), and the Hunan Provincial Innovation Foundation for Postgraduate, China (Grant No. CX2011B033).

†Corresponding author. E-mail: zhoumeng6806@163.com

© 2012 Chinese Physical Society and IOP Publishing Ltd

2. Theory

When there are three frequencies, f_i, f_j, and f_k, in the fiber, a new frequency $f_{ijk} = f_i + f_j - f_k$ will be generated through the FWM process. FWM is easier to occur for $f_i = f_j$ which corresponds to the partially degenerate case. The phase mismatch of the partially degenerate FWM can be approximately expressed as[1,18,19]

$$\kappa \approx \beta_2 \omega_s^2 + 2\gamma P, \tag{1}$$

where β_2 is the group velocity dispersion (GVD) parameter, ω_s is the angular frequency spacing, γ is the nonlinear coefficient, and P is the pump power. The first and second terms represent the GVD and nonlinear contributions respectively. If the pump power is low, the second term is negligible. However, its influence cannot be ignored for a high power due to the nonlinearity. In addition, the second term is always positive, so the phase-matching condition can only be satisfied for $\beta_2 < 0$, i.e., the anomalous dispersion. It has been indicated that MI resulting from FWM occurs when $\kappa = 0$ is achieved for a proper pump power. In particular, when the channel spacing coincides with the MI frequency, MIR emerges, which induces enhanced FWM interactions and accordingly rapid signal depletion because of efficient energy transfer to the sidebands. In addition, even if the phase is not rigorously matched, i.e., $\kappa \neq 0$, we can also define a coherence length as $L_{\rm coh} = 2\pi/|\kappa|$ and FWM still occurs efficiently for $L < L_{\rm coh}$, which is the so-called quasi-phase-matching condition.

3. Experiments

The experimental setup is shown in Fig. 1. The light from a laser diode (LD1) with 1549.26-nm wavelength and $\sim$ 5-mW output power was amplified by a tunable erbium-doped fiber amplifier (EDFA1) before injected into an acoustic-optic modulator (AOM) due to its insertion loss of as high as $\sim$ 7 dB. The CW was turned into pulses by the AOM with its driver connected to an arbitrary function generator (AFG), which supplies a 100-ns pulse signal with the duty cycle of 1%. The pulses were amplified again by a pulse EDFA (EDFA2) to achieve a power high enough to induce MI and then filtered by an optical filter with $\sim$ 0.3-nm bandwidth to suppress the amplified spontaneous emission (ASE) noise of the EDFAs. Three isolators (ISO1, ISO2, ISO3) are used to avoid the return light to protect LD1, AOM, and EDFA2, respectively. Lights from this optical path as well as another LD (LD2) whose wavelength and output power can be tuned are coupled into the 25-km SMF by a 3-dB coupler. The spacing between the two signal channels can be changed by adjusting the wavelength of LD2 and the output spectra can be observed by an optical spectrum analyzer (OSA).

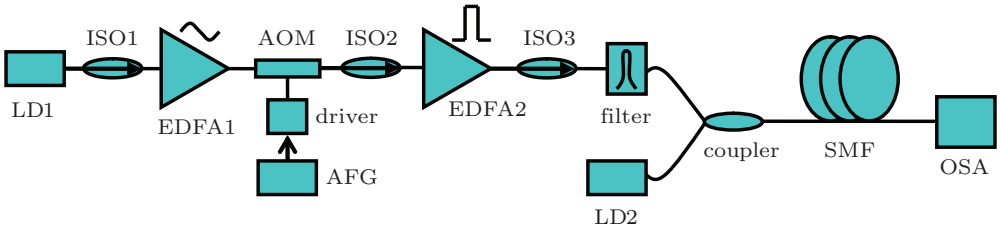


Fig. 1. (colour online) The experimental setup. LD: laser diode, ISO: isolator, EDFA: erbium-doped fiber amplifier, AOM: acoustic-optic modulator, AFG: arbitrary function generator, SMF: single-mode fiber, OSA: optical spectrum analyzer.

It should be noted that, for 100-ns pulses, MI responds to the peak power due to $\sim$10-fs response time,[20] while stimulated Brillouin scattering (SBS), another important nonlinear effect whose threshold is as low as $\sim$ 5.7 mW for 25-km SMF (according to our measurement data), responds to the average power due to $\sim$ 10-ns response time which is close to the used pulse width.[1] Therefore, we ensure the average power below the SBS threshold to exclude its influence in the experiments. In addition, we use the oscillograph to observe the input pulse shape of the SMF, and divide the peak voltage by the conversion efficiency of the photodetector to obtain the input peak power.

4. Results and discussion

The output spectra at different channel spacings are shown in Fig. 2. The peak power of the pulse is fixed at $\sim$ 89.6 mW after the coupler and the CW power is $\sim$ 1.7 mW at the same location. The wavelength of the pulse is fixed at 1549.26 nm. Supposing $\beta_2 = -20$ ps^2/km and $\gamma = 2$ W^{-1}·km^{-1} and using $\kappa = 0$, we can obtain $f_{\rm MI} = 21.3$ GHz (0.17 nm), a little higher than that in Fig. 2 (0.13 nm), which can be attributed to the fiber attenuation.[15] At first, we ensure the channel spacing is close to but not the same as $f_{\rm MI}$, as shown in Fig. 2, corresponding to 0.27, 0.22, and 0.18 nm, respectively, which are a little higher than 0.13 nm. For convenience, we label the pulse and CW channel as channels 1 and 2 respectively. It is apparent that the f_{112} components appear with the absence of f_{221}. Although the phase-matching condition is not precisely satisfied, the coherence lengths of the above three cases can be calculated to be 12, 27, and 155 km for the f_{112} components, which are long enough for FWM to occur effectively. It can be also found that the f_{112} power decreases with the increasing channel spacing, i.e., the decreasing coherence length, which verifies the quasi-phase-matching condition mentioned above.

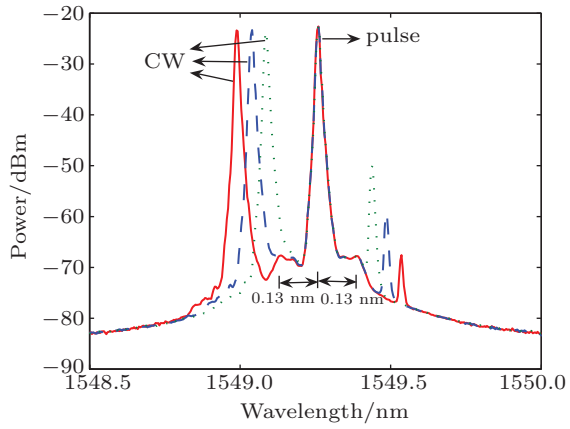


Fig. 2. (colour online) Output spectra of a CW and a pulse for different channel spacings.

To make a comparison, we present the output spectra when channel 1 is also a CW in Fig. 3, and the two CW powers are both $\sim$ 1.7 mW, which are the same as Fig. 2. Obviously, both f_{112} and f_{221} are present at this time, which is different from Fig. 2. We can explain this phenomenon as follows: In the presence of two-channel transmission, there exists competition between f_{112} and f_{221} through the FWM process. For the case of Fig. 2, the generation of f_{112} takes priority of f_{221} due to a much longer coherence length of the quasi-phase-matching condition caused by the high peak power of channel 1. As a result, most of the power is transferred to f_{112}, suppressing the generation of f_{221}. However, for the case of Fig. 3, the powers of the two channels are close to each other and the competition abilities of f_{112} and f_{221} are comparative, leading to the coexistence of the two components with almost the same power, which is essentially due to the energy exchange among different channels.[21] From the above discussion, we can propose a method to select the FWM-induced sidebands for the two-channel transmission, which is based on the proper utilization of a CW as well as a pulse. We hope it will have potential applications in the scopes of frequency conversion and sideband suppression.

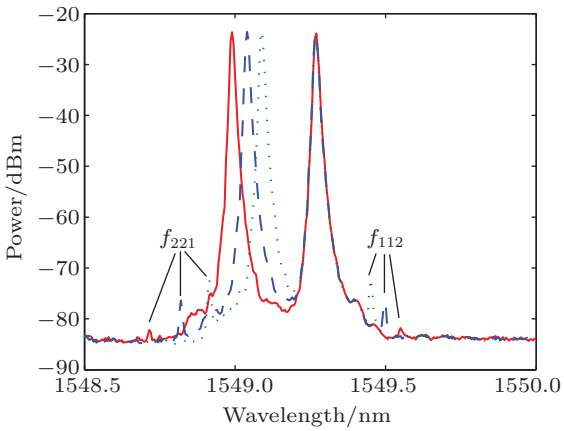


Fig. 3. (colour online) Output spectra of two CWs for different channel spacings.

Keeping the pulse and CW powers unchanged and adjusting the channel spacing within the MI frequency range, we can obtain the MIR output spectra, as shown in Figs. 4 and 5. It can be found that, with the matched phase, MIR enhances the efficiency of the FWM interactions, leading to the generation of the second-order sidebands. Taking Fig. 4 as an example, the f_{112} component is firstly generated due to the phase-matching condition and we label it as channel 3. Then the second-order FWM processes occur, which induce the f_{132} and f_{331} components on the right channel of channel 3, and the f_{123} component on the left channel of the CW channel (channel 2). Of course, this left channel also includes the first-order f_{221} component. A more detailed analysis about this multiple FWM processes can be found in Ref. [22]. Signal depletion is considerably severe because of the efficient energy transfer to the four sidebands (counting the CW in), which causes the decreasing of the

signal-to-noise ratio (SNR) and limits the transmission length of the fiber systems. Furthermore, the spectra are broadened to a great extent due to MIR. Considering that the phase noise originates from the laser linewidth, it will be highly increased as a result of spectral broadening, which is harmful to the interferometric fiber sensing system as the detection resolution decreases with the phase noise. Therefore, it is necessary to avoid the occurrence of MIR in many practical applications.

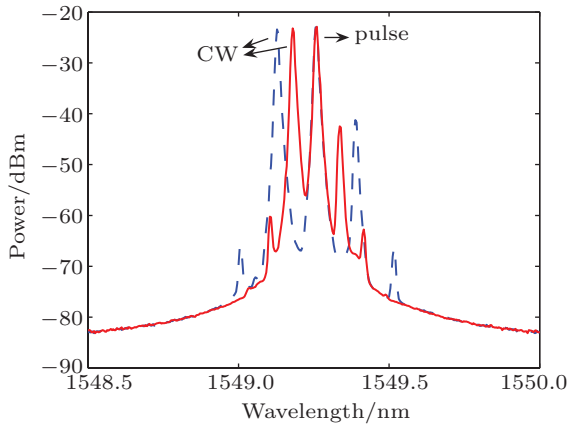


Fig. 4. (colour online) Output spectra in the MIR region with the CW on the left of the pulse.

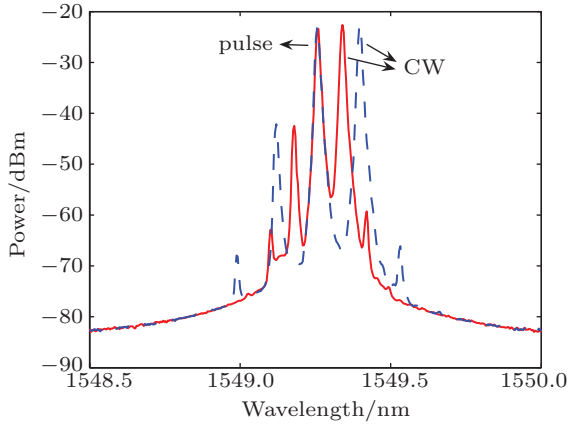


Fig. 5. (colour online) Output spectra in the MIR region with the CW on the right of the pulse.

Keeping the pulse power unchanged and fixing the CW frequency at 1549.38 nm, i.e., the channel spacing of 0.12 nm within the MI frequency, we change the CW power (measured after the coupler) to investigate the variations of MIR, as shown in Fig. 6. It can be found that both the number and the power of the sidebands increase with the input CW power. In the MIR process, the CW acts as a seed light and efficient energy transfer is realized through the MI induced FWM. To see this more clearly, we present the output power of the seed light as well as the sidebands versus the input CW power in Fig. 7. We label the sideband which is the nearest to the pump pulse in the shorter wavelength region of Fig. 6 as sideband 1, and in the same way we can label sidebands 2 and 3, etc. It is easy to find that the sideband number increases from 1 to 3 with the input CW power (from 2 to 6 in the whole spectra including the seed light), and the powers of the sidebands follow the variation of the seed light. Therefore, increasing the seed power will enhance the MIR efficiency, which should be avoided in practical applications.

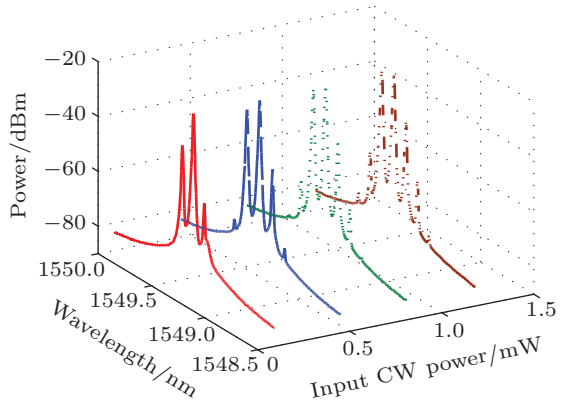


Fig. 6. (colour online) Output spectra for different input CW powers.

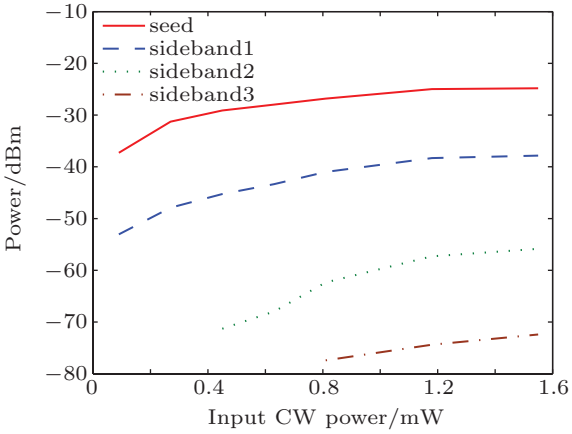


Fig. 7. (colour online) Powers of the seed and sidebands versus input CW power.

Fixing the CW power and frequency at 0.09 mW and 1549.38 nm, respectively, we change the peak power of the input pulse (measured after the coupler) by adjusting the gain of EDFA1 to investigate the variations of MIR. To make a comparison, we present the

output spectra without and with the CW at the input peak powers of 73.8, 81.8, 85.6, and 89.4 mW, as shown in Figs. 8 and 9, respectively. It can be found in Fig. 8 that MI gradually becomes obvious as the input peak power increases. In addition, the power of the sideband increases with the input peak power, which is clearly shown in Fig. 9. Therefore, increasing the peak power of the pump pulse will also enhance the MIR efficiency because of more efficient energy transfer.

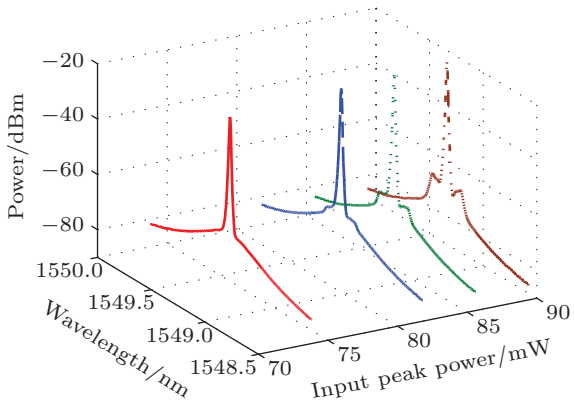


Fig. 8. (colour online) Output spectra of a pulse for different input peak powers.

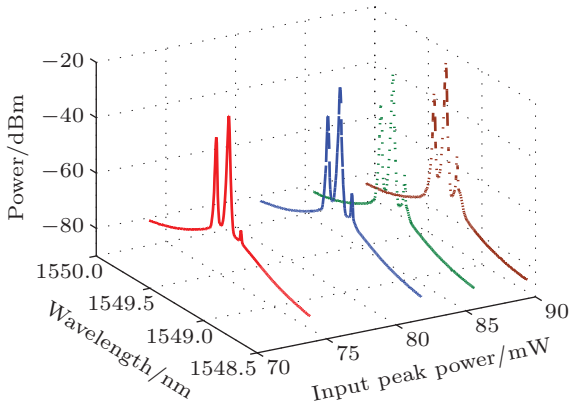


Fig. 9. (colour online) Output spectra of a CW and a pulse for different input peak powers.

As is well known, pulses are widely used in fiber communication and sensing systems, whose peak power reaches typically 200–300 mW in the latter case.[23] Using the phase-matching condition of FWM, we can obtain the MI frequency range between ∼ 30 GHz and ∼ 40 GHz for 1.55-μm transmission in the SMF (The actual values may be slightly smaller due to the fiber attenuation). At the same time, the channel spacing varies from 10 GHz to 100 GHz in the common WDM systems.[1] Therefore, to prevent the MIR-induced system performance degradation, we must exclude the special MI frequency from the applied channel spacing range. In Ref. [15], the DSF is used and the actual MI frequency is 87.5 GHz, which is higher than the case of usual SMF due to a lower fiber dispersion. Moreover, we can use a fiber with normal dispersion at the operation wavelength to suppress MI as well as MIR.[24]

5. Conclusion

In conclusion, we have investigated MI-induced FWM in the presence of MIR in the SMF from the phase-matching point of view. We used a CW and a pulse as light sources of the two channels. It is found that FWM-induced sidebands can be selected by this method, which can be explained using the quasi-phase-matching condition. The power of the generated sideband decreases with the channel spacing because of the decrease of the coherence length. It is also found that more sidebands are generated in the MIR region. In addition, the power of the sidebands increases with not only the peak power of the pump pulse but also the CW power acting as a seed, which is due to the efficient energy transfer through the MI-induced FWM. Considering that MIR causes severe performance degradation of the fiber communication and sensing systems which apply the WDM technology, the obtained results will play a key role in the practical applications of such systems.

References

[1] Agrawal G P 2001 *Nonlinear Fiber Optics* (New York: Academic Press)
[2] Inoue K, Nakanishi K, Oda K and Toba H 1994 *IEEE J. Lightwave Technol.* **12** 1423
[3] Ito Y, Onishi J, Kojima S and Numai T 2008 *Opt. Commun.* **281** 4515
[4] Forghieri F, Tkach R W and Chraplyvy A R 1995 *IEEE J. Lightwave Technol.* **13** 889
[5] Chang K D, Yang G C and Kwong W C 2000 *IEEE J. Lightwave Technol.* **18** 2113
[6] Yuan J H, Sang X Z, Yu C X, Xin X J, Li S G, Zhou G Y and Hou L T 2010 *Chin. Phys.* B **19** 074218
[7] Xin X J, Ma J X, Zhang Q, Deng C G, Wang K R, Yu C X and Liu B 2009 *Chin. Phys.* B **18** 3449
[8] Wang Y B, Xiong C L, Hou J, Lu Q S, Peng Y and Chen Z L 2011 *Acta Phys. Sin.* **60** 014201 (in Chinese)
[9] Yin J C, Xiao X S and Yang C X 2010 *Acta Phys. Sin.* **59** 3986 (in Chinese)
[10] Shibata N, Braun R P and Waarts R G 1987 *IEEE J. Quantum Electron.* **QE-23** 1205

[11] Grosz D F, Chavez Boggio J M and Fragnito H L 1999 *Opt. Commun.* **171** 53
[12] Grosz D F and Fragnito H L 1998 *Microwave Opt. Technol. Lett.* **19** 149
[13] Foaleng S M and Thévenaz L 2011 *Proc. SPIE* **7753** 77539V
[14] Grosz D F and Fragnito H L 1998 *Microwave Opt. Technol. Lett.* **18** 275
[15] Grosz D F, Mazzali C, Celaschi S, Paradisi A and Fragnito H L 1999 *IEEE Photon. Technol. Lett.* **11** 379
[16] Liu X M 2011 *J. Lightwave Technol.* **29** 179
[17] Liu X M 2010 *Laser Phys.* **20** 842
[18] Yamamoto T and Nakazawa M 1997 *IEEE Photon. Technol. Lett.* **9** 327
[19] Yamamoto T and Nakazawa M 1999 *Electronics and Communications in Japan* (Part 2) **82** 148
[20] Zhu Y, Cabrera-Granado E, Calderon O G, Melle S, Okawachi Y, Gaeta A L and Gauthier D J 2010 *J. Opt.* **12** 104019
[21] Liu X M, Yang X F, Lu F Y, Ng J H, Zhou X Q and Lu C 2005 *Opt. Express* **13** 142
[22] Liu X M 2008 *Phys. Rev.* A **77** 043818
[23] Alasia D, González Herráezb M, Abrardia L, Lópezb S M and Thévenaza L 2005 *Proc. SPIE* **5855** 587
[24] Alahbabi M N, Cho Y T, Newson T P, Wait P C and Hartog A H 2004 *J. Opt. Soc. Am.* B **21** 1156